Identification of the Attainable Region for Batch Reactor Networks

Benjamin J. Davis, Larry A. Taylor, and Vasilios I. Manousiouthakis*

Department of Chemical and Biomolecular Engineering, University of California, Los Angeles, California 90095

In this work, we describe a method for automatically identifying the set of all points in concentration space that represent outlet compositions of some network of discretely fed batch reactors for a given reaction set with known kinetics. This so-called batch attainable region (BAR) is dependent on the batch network's feed and total operating time, and it is shown to be quantifiable using the Infinite DimEnsionAl State-space (IDEAS) framework. We first establish that a simple batch reactor model possesses the properties that allow application of the IDEAS framework. We then formulate the resulting IDEAS Infinite Linear Program (ILP) whose solution is guaranteed to identify the globally optimal network of batch reactors. We subsequently use a simple transformation of this IDEAS ILP that leads us to propose two algorithms that are related to the construction of the true BAR. The first is a "Shrink-Wrap"-like algorithm that is similar to that previously reported [Manousiouthakis et al. The Shrink-Wrap Algorithm for the Construction of the Attainable Region: Application of the IDEAS Framework. *Comput. Chem. Eng.* **2004**, *28*, 1563] and creates increasingly accurate approximations of a set guaranteed to contain the true BAR for all network operating times. The second is a breadth-first algorithm that creates increasingly accurate inner approximations to the BAR for a given network operating time. These two algorithms are applied to an example from the literature and are shown analytically to converge in the limit to the true BAR.

Introduction

Evaluation of limits on the performance of reactors and reactor networks is crucial to the economic success of any chemical process network. Consequently, the analysis and design of reactors and reactor networks have been the primary foci of process systems engineering research. Previous works on non-steady-state reactor networks have addressed techniques for analyzing, modeling, or optimizing single-batch units, but they make little mention of how units can be used in conjunction or what theoretical limits exist on the performance of these types of non-steady-state systems. Because non-steady-state networks are fundamentally different from their steady-state counterparts, identification of these performance limits requires careful consideration of the effect of time (both reaction and holding time) and causal relationships between reactors.

The goal of this work is to apply the Infinite DimEnsionAl State-space (IDEAS) framework to construction of the batch attainable region (BAR) for non-steady-state networks of batch reactors; this is the first application of IDEAS to a network of dynamic process units. The remainder of the work is structured as follows: first, we give background information on reactor network synthesis (RNS), the IDEAS conceptual framework, and attainable region (AR) construction. Next, the applicability of IDEAS to batch RNS is established and the relevant IDEAS infinite linear program (ILP) is formulated. We then outline a variable transformation which leads to two algorithms that are related to the construction of the true BAR: the first is similar to the "Shrink-Wrap" algorithm that was developed by Manousiouthakis et al.[1] for the construction of the steady-state AR and creates increasingly accurate approximations of a set guaranteed to contain the true BAR for all network operating times. The second is a breadth-first algorithm that creates increasingly accurate inner approximations to the BAR for a given network operating time. These two algorithms are applied to an example from the literature and are shown to converge in the limit to the true BAR.

* To whom correspondence should be addressed. Tel.: 310 206 0300. Fax: 310 206 4107. E-mail address: vasilios@ucla.edu.

Background

Automatic (computer-based) reactor network synthesis (RNS) evolved as a field of its own starting in the 1980s. Chitra and Govind[2] performed work in 1981 on the identification of optimal reactor types and configurations using a super-structure-based approach. They later expanded on their earlier work, applying a superstructure-based method for optimal RNS for both isothermal[3] and non-isothermal[4] reaction systems. Ong[5] considered the optimization of continuously stirred tank reactors (CSTRs) in series using Bellman's[6] dynamic programming. Pibouleau et al.[7] proposed a mixed-integer nonlinear programming (MINLP) formulation for the automatic synthesis of networks featuring CSTRs and single-stage separation units. In 1994, Omtveit et al. presented a RNS method that also included a separation network as a separate sub-problem;[8] that paper also gives an extensive literature review of work on RNS to that point. Smith and Pantelides[9] gave another reactor−separator network superstructure-based formulation in their 1995 work. Bikic and Glavic produced a series of papers on a superstructure-based nonlinear programming (NLP) method for RNS for networks with multiple multicomponent feeds,[10] non-isothermal complex reaction schemes,[11] and reactor/separator networks.[12] Their 1996 work stated that "the proposed design procedure can also be used to support the design of batch processes", but that work did not specifically address the claim. Esparta et al.[13] proposed a superstructure-based method for RNS using isothermal two-phase CSTRs in 1998. Hua et al. proposed a NLP model for RNS that included "differential recycling DSR" reactor units.[14] Mehta and Kokossis[15] proposed a stochastic optimization approach to non-isothermal and multiphase RNS. Pahor et al. proposed a superstructure/MINLP approach for optimization[16] and then, in later work, applied the method to the non-isothermal production of allyl chloride.[17] Moreover, in 1999, Grossman et al. gave a review of advances in mathemati-

10.1021/ie071664l CCC: $40.75
Published on Web 04/23/2008 **PAGE EST: 13**

cal programming for process systems synthesis;[18] this review has sections devoted to both RNS and AR construction theory, respectively.

The RNS problem was also approached using the methods of optimal control; the work by Aris[19] was significant in this field, addressing the problem of optimal control of a batch reactor. In 1970, Paynter and Haskins[20] formulated an optimal control problem for determining the optimal reactor type for a single reactor using an axial dispersion model. Waghmare and Lim applied optimal control theory to single isothermal reactor systems[21] and later applied the same techniques to complex reaction schemes.[22] Achenie and Biegler[23−25] proposed an NLP method for RNS that used superstructures in a "target-based" approach. Godorr et al.[26] outlined optimal control policies for reactor structures on the AR boundary, using temperature as the control variable. Hillestad formulated the RNS problem as an optimal control problem and then examined its solution for the isothermal[27] and non-isothermal[28] cases.

The IDEAS conceptual framework was proposed by Manousiouthakis et al.[1] in an effort to overcome two limitations of superstructure-based optimal process network synthesis methods: (i) the considered superstructure may impose unforeseen limitations on the eventually obtained optimal network, and (ii) the nonconvex nature of the resulting superstructure-based optimization formulations (NLP, MINLP, etc.) only guarantees local optimality of the obtained optimal network. IDEAS overcomes these limitations by considering all possible process network configurations and establishing that most commonly applied process models can be used to yield optimization formulations with an infinite number of variables and an infinite number of linear constraints. The ability of IDEAS to address several long-standing process network synthesis problems has been demonstrated on the minimum utility cost (MUC) problem for mass exchange networks[29] (MENs), the minimum plate area[30] and MUC[31] problems for heat-integrated complex distillation networks, the minimum total annualized cost (MTAC) problem for separation networks[32] and power cycle networks,[33] the MUC problem for heat and power integrated complex distillation networks,[34] and the minimum total liquid hold-up problem for complex reactive distillation networks.[35]

The attainable region (AR) for a given set of reactions and reactor technologies is defined as the set of all points in concentration space that are attainable through reaction and mixing from a given feed point; this definition has been widely credited to Horn in 1964.[36] Quantification of the AR for reactor networks is an important problem in chemical process optimization, because knowledge of the AR quantifies, for process designers, the fundamental limitations on the performance of chemical process flowsheets. Identification of the particular reactor—or, more generally, the reactor network—whose output concentration vector is an extreme point of the AR is often the objective of reactor engineering studies. Work by Gavalas[37] in 1968 on nonlinear differential equations for chemical reactors introduced the concept of the invariant manifold and gives example two-dimensional (2D) plots of the conversion of different species. Many of the proposed AR construction methods in the literature are based on a geometric approach to AR identification that was outlined in the 1987 work by Glasser et al.[38] This geometric approach has spawned numerous other works whose objective was to identify the AR for adiabatic, variable density reactor networks,[39] segregated and maximum mixed reactor networks,[40] exothermic reversible reaction kinetics,[41] and reaction systems with external heating and cooling.[42]

In 1997, Feinberg and Hildebrandt[43] reported on the determination of the optimal reactor network configuration using the geometric properties of the AR extreme points in the first part of a three-part series. This work was later expanded by Feinberg in 1999 to a more extensive set of mathematical properties of the AR boundary[44] and in 2000 to properties of critical DSRs[45] and CSTRs[46] whose outlets are on the AR boundary. In 1999, McGregor et al.[47] examined the relationship between the geometric AR identification method and Pontryagin's maximum principle. Rooney et al.[48] extended the geometric AR identification method to higher dimensions by extending the 2D subspace. In 1997, Nisoli et al.[49] outlined a method for identifying the AR for a two-phase reaction−separation system; they applied the method to the production and separation of dimethyl ether (DME) from methanol and methyl *tert*-butyl ether (MTBE) from isobutene and methanol. That same year, Smith and Malone[50] outlined an application of AR identification in the free-radical polymerization of poly(methyl methacrylate) (PMMA). Later, in 2002, Gadewar et al.[51] analyzed networks of two-phase CSTRs that are surrogates for reactive distillation units to find an AR for such networks. Kauchali et al.[52] used the earlier methods of Nisoli et al.[67] to identify candidate ARs for the water-gas shift (WGS) reaction, which is a problem that also was previously studied by Omtveit et al.[53]

More recently, the IDEAS conceptual framework has also been applied in the construction of the AR for reactor networks. Burri et al.[54] first presented several IDEAS-based infinite linear programming (ILP) formulations of the AR construction problem in 2002. That same year, Kauchali et al.[55] independently developed an IDEAS-like linear programming model for extending candidate ARs. Manousiouthakis et al.[1] then presented properties of one of the aforementioned IDEAS ILPs, which allowed construction of the true AR without explicit solution of the ILP using a so-called "Shrink-Wrap" algorithm. Concurrent and independent work by Abraham and Feinberg[56] proposed a method of bounding hyperplanes to identify subsets of a superset containing the AR that are guaranteed not to contain the AR. More recently, Zhou and Manousiouthakis demonstrated that variants of the Shrink-Wrap algorithm are applicable to the AR construction for nonideal axial dispersion reactor models[57] and variable-density fluid reactor models,[58] respectively.

There is extensive work in the literature that addresses single-batch reactor optimization and batch process scheduling. Rippin[59] gave a review of studies of individual batch units and their optimization in 1983. That same year, he also wrote an overview of general structures for batch process systems.[60] He followed up these reviews 10 years later with the current progress in the field of engineering and design of batch processes.[61] Reklaitis[62] gave a review of progress and issues in computer-aided batch process design in 1990. Levien[63] wrote on the optimal design of batch, discrete semi-batch, and continuous semi-batch reactor units in his 1992 work. Terwiesch et al.[64] surveyed industry needs for batch processes and suggested both optimal control methods for improvements and also further research problems to be addressed. Yi and Reklaitis[65] have performed work on the optimal synthesis of batch storage networks for chemical processes. Maravelias[66] examined the problem of optimal scheduling of single-stage and multistage batch processes using a mixed-integer sequencing algorithm. Later work by Sung and

Maravelias[67] defines a "process attainable region" for production planning and scheduling problems with limited equipment capacity.

Application of IDEAS to Batch Reactor Network Synthesis

The fundamental difference between batch and steady-state reactor network synthesis problems is the time dependence of the underlying batch reactor process. In a network context, this time dependence immediately raises the issue of "causality"; in a batch reactor network, a reactor cannot "feed" another reactor unless its contents are unloaded before the other reactor's loading time. To examine causality in a straightforward manner, we consider that batch reactor loading, unloading, and mixing operations can only occur at prespecified discrete times, $\{t_0, t_1, t_2, ..., t_n\}$ and are instantaneous. For the remainder of this work we will refer to the reactor inlet and outlet volumes (which are equal, because of our assumption of constant density) as flow rates; this is a slight misnomer, because each reactor's inlet and outlet are discrete (i.e., there is no temporal nature to the flow into or out of a reactor), but the convention of calling them flow rates makes the analogy between batch reactor networks and other steady-state reactor networks clearer. The inlet and outlet volumes of a batch reactor unit are extensive properties that do not affect the units' intensive properties, such as species concentrations, temperature, pressure, etc.

The standard model for a batch reactor is outlined in almost any reaction engineering textbook (see the work of Levenspiel,[68] Froment and Bischoff,[69] Schmidt,[70] Fogler,[71] Nauman,[72] Rawlings,[73] etc.). More recently, there have been more-complicated batch reactor models proposed in the literature that account for imperfect mixing and continuously fed batch operation;[74] however, we will not specifically address these complications in this work. To apply IDEAS to the batch reactor network synthesis problem, we must first prove that the batch reactor model is flow-invariant with respect to its intensive properties. Second, we must prove that the operations of mixing and splitting in the distribution network are linear. A more formal mathematical method for showing the applicability of IDEAS to a unit model has been previously outlined in Zhou et al.[57] We define our IDEAS inlet−outlet information map (M) for the batch reactor model as follows:

$$u = [\bar{C}(1)\ \ \bar{C}(2)\ \ ...\ \ \bar{C}(N)\ \ t^{in}\ \ t^{out}\ \ \lambda\ \ \bar{F}\,] \xrightarrow{M} y = [C(1)\ \ C(2)\ \ ...\ \ C(N)\ \ F\,] \quad (1)$$

$$\text{if } \lambda = 1\text{:}\quad \frac{d\hat{C}_i(t)}{dt} = R_i(\hat{C}_1(t), \hat{C}_2(t), ..., \hat{C}_i(t) ..., \hat{C}_N(t)) \quad \forall i = 1, ..., N \quad (2)$$

$$\text{if } \lambda = 1\text{:}\quad \bar{C}(i) \equiv \hat{C}_i(t^{in}) \qquad \forall i = 1, ..., N \quad (3)$$

$$\text{if } \lambda = 1\text{:}\quad C(i) \equiv \hat{C}_i(t^{out}) \qquad \forall i = 1, ..., N \quad (4)$$

$$\text{if } \lambda = 1\text{:}\quad \hat{C}_i(t) \geq 0 \qquad \forall i = 1, ..., N;\quad \forall t = [t^{in}, t^{out}] \quad (5)$$

$$\text{if } \lambda = 0\text{:}\quad C(i) = \bar{C}(i) \qquad \forall i = 1, ..., N \quad (6)$$

where u is the reactor inlet information vector, y the reactor outlet information vector, M the nonlinear reactor information input−output map, $\bar{C}_i(t)$ the concentration of species i in the reactor at time t, R_i the rate of generation of species i (in units of moles per volume per unit time), $\bar{C}(i)$ the concentration of species i in the reactor inlet, $C(i)$ the concentration of species i in the reactor outlet, t^{in} the reactor inlet time, t^{out} the reactor outlet time, λ the reactor technology flag, $\bar{F}$ the reactor volumetric "feed" (reactor volume), F the reactor volumetric "effluent" (constant density, $F = \bar{F}$), and N the number of species considered.

The "reactor technology flag" (λ) is a convention that is used to allow holding tanks to be part of the formulation. If $\lambda = 1$, the unit is a batch reactor with nonzero R_i defined by model eqs 2−5. If $\lambda = 0$, there is no reaction and the unit is a holding tank that is defined by eq 6 with holding time $t^{out} - t^{in}$. For IDEAS to be applied to this model, we must the identify vectors u_1, u_2, y_1, and y_2 and information maps M_1 and M_2 (which, together, comprise M) that satisfy the following properties:

$$\text{M:}\quad u = \begin{bmatrix} u_1 \\ u_2 \end{bmatrix} \rightarrow y = \begin{bmatrix} y_1 \\ y_2 \end{bmatrix} = \begin{bmatrix} M_1(u_2) \cdot u_1 \\ M_2(u_2) \end{bmatrix} \quad (7)$$

We will define these vectors as follows:

$$u_1 = [\bar{F}] = [F] = y_1 \quad (8)$$

$$u_2 = [\bar{C}(1)\ \ \bar{C}(2)\ \ ...\ \ \bar{C}(N)\ \ t_{in}\ \ t_{out}\ \ \lambda\,] \quad (9)$$

$$y_2 = [C(1)\ \ C(2)\ \ ...\ \ C(N)\,] \quad (10)$$

Because $y_1 = u_1$, the map M_1 is just the identity map. We uniquely define the map M_2 by assuming in this work that the set of differential equations in eq 2 with initial conditions in eq 3 admits a solution and that the solution is unique. Sufficient conditions on the properties of the rate vector for this to be true can be found in theorem 2.4 of Khalil.[75] Each of the outlet concentrations can be found using the information in u_2; therefore, we can define the map M_2 as follows:

$$M_2\text{:}\quad u_2 \xrightarrow{\text{eqs 2−6}} y_2$$

Therefore, this batch reactor model satisfies the first necessary property for the applicability of the IDEAS framework. The second property—that the operations of mixing, splitting, and recycle are linear—is obvious, given that the intensive properties of the units are considered to be known.

Graphical Representation of Batch Reactor Networks

As an example, consider a simple batch reactor network that consists of three reactors and two holding tanks. Reactor 1 is fed at some initial time (we will call it t_0) and runs until its outlet time t_1. At that time, the reactor 1 outlet is split into three parts, which are fed into reactor 2, reactor 3, and holding tank 1, respectively. Reactor 2 operates from t_1 (which is the output time of reactor 1) until time t_2 and then its output enters holding tank 2. Reactor 3 operates from t_1 until t_3, at which time its outlet is mixed with the contents of holding tanks 1 and 2 to form the network outlet. This simple batch reactor network can be visualized in a time-axis form, as shown in Figure 1.

We can also represent this same process flowsheet in an OP/DN form, by rearranging the process network diagram such that all the mixing and splitting operations are contained in the distribution network (DN) and all unit operations (the three batch reactors and two holding tanks) are contained in the operator block (OP). This method of representing a flowsheet can be used to best visualize the IDEAS formulation of the batch reactor network problem. In the IDEAS formulation, all possible reactors are considered in the formulation of the optimization problem; therefore, instead of a diagram with three reactors, there is an infinite number of batch reactors and holding tanks

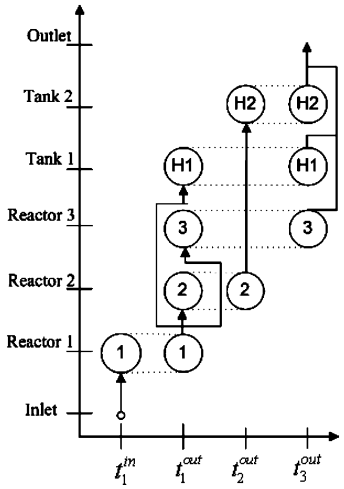

Figure 1. Batch reactor network flowsheet in time axis form.

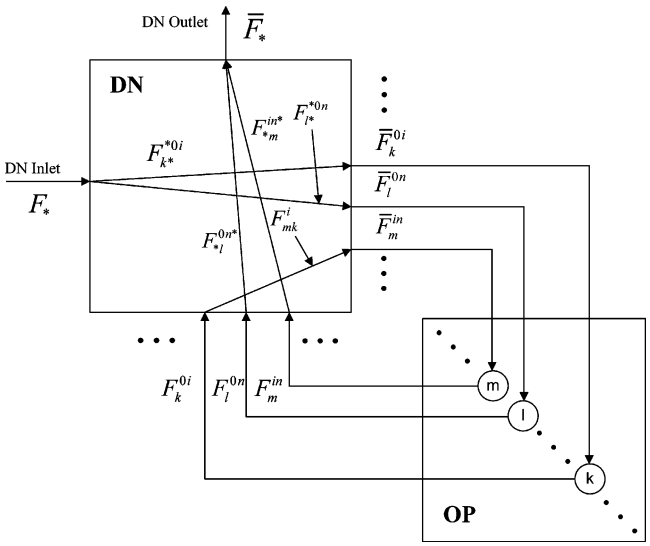

Figure 2. IDEAS representation for batch reactor network problem.

Table 1. Definition of Symbols Used in Figure 2

variable	definition
$\bar{F}_*$	flow out of the DN/overall network
F_*	flow into the DN/overall network
$\bar{F}_m^{ij}$	flow into the *m*th reactor/holding tank, operating from time t_i until time t_j
F_l^{ij}	flow out of the *l*th reactor/holding tank, operating from time t_i until time t_j
F_{ml}^{ijk}	flow from the *l*th reactor/holding tank, which operates from time t_i until time t_j to the *m*th reactor/holding tank which operates from time t_j until time t_k
F_{m*}^{*0k}	flow from DN inlet to the *m*th reactor/ holding tank, operating from time t_0 until time t_k
$F_{*l}^{in}*$	flow to DN outlet from the *l*th reactor/ holding tank, operating from time t_i until time t_n
$\bar{C}_m^{ij}$	property vector for the flow $\bar{F}_m^{ij} = [\bar{C}_m^{ij}(1)\ \bar{C}_m^{ij}(2) \ldots \bar{C}_m^{ij}(N)]^T$
C_l^{ij}	property vector for the flow $F_l^{ij} = [C_l^{ij}(1)\ C_l^{ij}(2) \ldots C_l^{ij}(N)]^T$
$\bar{C}_*$	property vector for the DN outlet $= [\bar{C}_*(1)\ \bar{C}_*(2) \ldots \bar{C}_*(N)]^T$
C_*	property vector for the DN inlet $= [C_*(1)\ C_*(2) \ldots C_*(N)]^T$

included in OP as in Figure 2. The variables shown in Figure 2 are defined in Table 1.

Note that (i) the network outlet and all reactors in the network may only be fed at their designated inlet time, (ii) the network inlet time is arbitrarily designated as t_0, and (iii) the network outlet time is t_n. Thus, n designates the number of times that the reactor/holding tank contents are allowed to mix ($n = 3$ in the example above). Also note that holding tanks are implicitly included in this formulation as units in the OP block (no holding occurs in the DN).

IDEAS ILP Formulation for Batch Reactor Network Synthesis

The IDEAS optimization problem outlined below considers every possible reactor and holding tank unit and all causally feasible interconnections in the DN, thereby guaranteeing that all possible batch reactor networks are included in the mathematical problem formulation. Without any loss of generality, each unit's input information vector u_2 is considered to be known, and thus, using the information map M, its output information vector y_2 is also known. Knowledge of each unit's input and output information vectors y_2 and u_2 will be shown below to lead to an IDEAS formulation of the optimal batch reactor network synthesis (RNS) problem that is an infinite linear program (ILP). Before we can outline this IDEAS ILP, we first define (infinite) sets of reactors that are organized by their inlet and outlet times:

$$\mathrm{S}^{ij} \equiv \text{the set of all reactors and holding tanks that operate from time } t_i \text{ to time } t_j \quad (11)$$

Using these sets as defined, the formulation for the batch reactor network synthesis problem can be set up as follows:

$$\text{minimize } v = f(F_{m*}^{*\,0k}, F_{*l}^{in}, F_{ml}^{ijk}, F_m^{ij}, \bar{F}_m^{ij})$$

subject to:

(1) Distribution Network Inlet Mass Balance (Splitting)

$$F_* = \sum_{k=1}^{n} \sum_{m \in \mathrm{S}^{0k}} F_{m*}^{*\,0k} = \sum_{k=1}^{n} \sum_{m \in \mathrm{S}^{0k}} \bar{F}_m^{0k} = \sum_{k=1}^{n} \sum_{m \in \mathrm{S}^{0k}} F_m^{0k}$$

(2) OP Outlet Mass Balances (Splitting)

$$F_m^{ij} = \sum_{\substack{k=2 \\ k>j>i}}^{n} \sum_{l \in \mathrm{S}^{jk}} F_{lm}^{ijk}$$

$$\forall m \in \mathrm{S}^{ij};\ \forall i = 0, \ldots, n-2;\ \forall j = 1, \ldots, n-1\ (i < j)$$

(3) Distribution Network Outlet Mass Balance (Mixing)

$$\bar{F}_* = \sum_{i=0}^{n-1} \sum_{l \in \mathrm{S}^{in}} F_{*l}^{in}* = \sum_{i=0}^{n-1} \sum_{l \in \mathrm{S}^{in}} F_l^{in}$$

(4) Distribution Network Outlet Component Balances (Mixing)

$$\bar{C}_* \bar{F}_* = \sum_{i=0}^{n-1} \sum_{l \in \mathrm{S}^{in}} C_l^{in} F_{*l}^{in}* = \sum_{i=0}^{n-1} \sum_{l \in \mathrm{S}^{in}} C_l^{in}\, F_l^{in}$$

(5) OP Inlet Mass Balances (Mixing)

$$\bar{F}_m^{jk} = \sum_{\substack{i=0 \\ i<j<k}}^{n-2} \sum_{l \in \mathrm{S}^{ij}} F_{ml}^{ijk}$$

$$\forall m \in \mathrm{S}^{jk};\ \forall j = 1, \ldots, n-1;\ \forall k = 2, \ldots, n\ (j < k)$$

(6) OP Component Balances (Mixing)

$$\bar{C}_m^{jk}\bar{F}_m^{jk} = \sum_{\substack{i=0 \\ i<j<k}}^{n-2} \sum_{l\in S^{ij}} C_l^{ij} F_{ml}^{ijk}$$

$$\forall m \in S^{jk};\ \forall j = 1, ..., n-1;\ \forall k = 2, ..., n\ (j < k)$$

(7) Positivity Constraints

$$\bar{F}_m^{ij} \geq 0, \quad F_m^{ij} \geq 0, \quad F_{lm}^{ijk} \geq 0 \quad \forall m \in S^{ij};\ \forall l \in S^{jk};$$
$$\forall i = 0, ..., n-2;\ \forall j = 1, ..., n-1;$$
$$\forall k = 2, ..., n\ (i < j < k)$$

$$F_{m^*}^{*\ 0k} \geq 0, \quad F_{*l}^{in*} \geq 0 \qquad \forall i = 0, ..., n-1;$$
$$\forall k = 1, ..., n;\ \forall m \in S^{0k};\ \forall l \in S^{in}$$

(8) Constant Density Assumption

$$F_m^{ij} = \bar{F}_m^{ij}, \quad F_* = \bar{F}_* \qquad \forall m \in S^{ij};\ \forall i = 0, ..., n-1;$$
$$\forall j = 1, ..., n$$

(9) Batch Reactor/Holding Tank Model Map

$$[\bar{C}_m^{ij}(1)\ \ \bar{C}_m^{ij}(2)\ \ ...\ \ \bar{C}_m^{ij}(N)\ \ t_i\ \ t_j\ \ \lambda_m^{ij}] \xrightarrow{M_2}$$
$$[C_m^{ij}(1)\ \ C_m^{ij}(2)\ \ ...\ \ C_m^{ij}(N)] \qquad \forall m = 1, ..., \infty;\ \forall i = 0, ..., n$$

$$\text{if } \lambda_m^{ij} = 1\text{: Batch Reactor, } R_i(\bar{C}_m^{ij}(i)) \neq 0 \qquad \forall i = 0, ..., N$$

$$\text{if } \lambda_m^{ij} = 0\text{: Holding Tank, } R_i(\bar{C}_m^{ij}(i)) = 0 \qquad \forall i = 0, ..., N$$

The aforementioned optimization problem is an ILP (because all unit inlet and outlet concentrations are known) as long as the objective function f is a linear function of the network's "flow" variables. The most commonly considered linear objective functions are maximization or minimization of one particular component's DN outlet concentration, maximization of selectivity or yield of a desired product, minimization of total network volume, etc.

In practice, this ILP is not solved directly; this would be impossible except for certain specific cases where a solution could be found analytically in the limit. Instead, finite linear programs (or LPs) are solved that give an approximation to the ILP's solution. As larger and larger LPs are solved, their solutions more accurately approximate the solution of the ILP. If we represent the number of units considered in our LP approximation as U and the associated objective function value for the LP as ν_U, then the infinite sequence

$$\{\nu_U\}_{U=1}^{\infty} \tag{12}$$

has been proven to be a non-increasing sequence of upper bounds on the actual ILP objective function value (ν_∞, or just ν) and the sequence is guaranteed to converge to ν (proof of this is given in work by Justanieah,[76] in collaboration with Manousiouthakis).

Definition of Mixing Ratios

Now that we have defined our problem above, we will introduce the concept of a mixing ratio, a_{ml}^{ijk}. A mixing ratio is a ratio between 0 and 1 (inclusive) that defines the fraction of a particular unit's inlet stream (or the network outlet) coming from another unit (or from the network inlet). Mixing ratios satisfy the following equations:

$$F_{ml}^{ijk} = \bar{F}_m^{jk} a_{ml}^{ijk} \tag{13}$$

$$0 \leq a_{ml}^{ijk} \leq 1 \tag{14}$$

$$\forall m \in S^{jk};\ \forall l \in S^{ij};\ \forall i = 0, ..., n-2;\ \forall j = 1, ..., n-1;\ \forall k = 2, ..., n\ (i < j < k)$$

Similar equations can be written for the OP inlet and network outlet mixing ratios:

$$F_{m^*}^{*\ 0k} = \bar{F}_m^{0k} a_{m^*}^{*\ 0k} \qquad \forall m \in S^{0k};\ \forall k = 1, ..., n \tag{15}$$

$$F_{*l}^{in*} = \bar{F}_* a_{*l}^{in*} \qquad \forall l \in S^{in};\ \forall i = 0, ..., n-1 \tag{16}$$

$$0 \leq a_{*l}^{in*} \leq 1 \qquad \forall l \in S^{in};\ \forall i = 0, ..., n-1 \tag{17}$$

To identify the BAR, we then introduce the following definitions:

Definition 1: Active unit − a unit (reactor or holding tank) is active if its volume (outlet flow rate) is nonzero (strictly positive) in the feasible solution to the above optimization problem.

Definition 2: Inactive unit − a unit is inactive if its volume is zero in the feasible solution to the above optimization problem.

Without any loss of generality, mixing ratios from inactive to active units can be set to zero, because flows to or from an inactive unit are zero. In addition, the sum of all mixing ratios that correspond to any unit inlet can be set to one. Indeed, for mixing ratios that correspond to active unit inlets, this must be the case, whereas for mixing ratios that correspond to inactive units, this assumption is inconsequential. Furthermore, constraint set 6 of the aforementioned IDEAS ILP is automatically satisfied for an inactive unit, while it suggests that the inlet concentration vector of an active unit fed at time t_j belongs to the convex hull of outlet concentration vectors of active units, which outlet at time t_j.

We also consider that these mixing ratios satisfy the following five conditions; these equations (eqs 18−22) are automatically satisfied for active units and are irrelevant to the IDEAS ILP formulation for units with zero flow, based on constraint sets 3, 5, and 6 in the above formulation:

$$\sum_{\substack{i=0 \\ i<j<k}}^{n-2} \sum_{l\in S^{ij}} a_{ml}^{ijk} = 1$$
$$\forall m \in S^{jk};\ \forall j = 1, ..., n-1;\ \forall k = 2, ..., n\ (j < k) \tag{18}$$

$$\sum_{i=0}^{n-1} \sum_{l\in S^{in}} a_{*l}^{in*} = 1 \tag{19}$$

$$\sum_{\substack{i=0 \\ i<j<k}}^{n-2} \sum_{l\in S^{ij}} C_l^{ij} a_{ml}^{ijk} - \bar{C}_m^{jk} = 0$$
$$\forall m \in S^{jk};\ \forall j = 1, ..., n-1;\ \forall k = 2, ..., n\ (j < k) \tag{20}$$

$$a_{m^*}^{*\ 0k} = 1 \qquad \forall m \in S^{0k};\ \forall k = 1, ..., n \tag{21}$$

$$\bar{C}_m^{0k} = C_* \qquad \forall m \in S^{0k};\ \forall k = 1, ..., n \tag{22}$$

We can substitute in these mixing ratios (eqs 13−17 above) into the feasible set of the IDEAS ILP to transform it to an

equivalent set. We also make use of the constant density assumption to eliminate some of the redundant flow variables and positivity constraints, reforming the set as follows:

1. $F_* = \sum_{k=1}^{n} \sum_{m \in S^{0k}} F_m^{0k} a_{m*}^{0k} = \sum_{k=1}^{n} \sum_{m \in S^{0k}} F_m^{0k}$

2. $F_m^{ij} = \sum_{\substack{k=2 \\ k>j>i}}^{n} \sum_{l \in S^{ik}} F_l^{jk} a_{lm}^{ijk}$

$$\forall m \in S^{ij};\ \forall i = 0, ..., n-2;\ \forall j = 1, ..., n-1\ (i < j)$$

3. $1 = \sum_{i=0}^{n-1} \sum_{l \in S^{in}} a_{*l}^{in*}$

4. $\bar{C}_* = \sum_{i=0}^{n-1} \sum_{l \in S^{in}} C_l^{in} a_{*l}^{in*}$

5. $1 = \sum_{\substack{i=0 \\ i<j<k}}^{n-2} \sum_{l \in S^{ij}} a_{ml}^{ijk}$

$$\forall m \in S^{jk};\ \forall j = 1, ..., n-1;\ \forall k = 2, ..., n\ (j < k)$$

6. $\bar{C}_m^{jk} = \sum_{\substack{i=0 \\ i<j<k}}^{n-2} \sum_{l \in S^{ij}} C_l^{ij} a_{ml}^{ijk}$

$$\forall m \in S^{jk};\ \forall j = 1, ..., n-1;\ \forall k = 2, ..., n\ (j < k)$$

7. $F_m^{ij} \geq 0, \quad 0 \leq a_{lm}^{ijk} \leq 1$

$$\forall m \in S^{ij};\ \forall l \in S^{jk};\ \forall i = 0, ..., n-2;\ \forall j = 1, ..., n-1;\ \forall k = 2, ..., n\ (i < j < k)$$

$$0 \leq a_{*l}^{in*} \leq 1$$

$$\forall i = 0, ..., n-1;\ \forall k = 1, ..., n;\ \forall m \in S^{0k};\ \forall l \in S^{in}$$

We have omitted the batch reactor model equations, because it is assumed that the infinite sequence of reactor inlet concentrations and their respective lambda parameters are known for a given reactor's inlet and outlet time, and thus all outlet concentrations are also known for each unit using the input−output map M. Also, this formulation assumes the positivity of the network inlet flow, because the problem would be trivial otherwise. All the constraints in the aforementioned set are linear, except for constraint set 2 (which corresponds to the OP outlet splitting mass balances).

Finite Approximation to Feasible Set

To approximately identify the solution to the aforementioned infinite problem, we discretize the concentration space with a finite number of grid points. We then consider all units with an inlet composition vector at one of the grid points, some at starting time t_i, and some at ending time t_j. Let U be the finite number of units that operate from each starting time t_i to each ending time t_j; we will define new finite sets G^{ij} with cardinality U, which approximate the infinite sets S^{ij}. The vector of all flows through each of these units in set G^{ij} can be defined as follows:

$$\mathbf{F}^{ij} = [F_1^{ij}\ \ F_2^{ij}\ \ F_3^{ij}\ \ \cdots\ \ F_U^{ij}]^{\mathrm{T}}$$

$$\forall i = 0, ..., n-1;\ \forall j = 1, ..., n\ (i < j) \quad (23)$$

$$A = \begin{bmatrix}
0 & A^{*01} & \dots & A^{*0n} & 0 & \dots & 0 & \dots & 0 & \dots & 0 & \dots & 0 & 0 & 0 \\
0 & 0 & \dots & 0 & A^{012} & \dots & A^{01n} & \dots & 0 & \dots & 0 & \dots & 0 & 0 & 0 \\
\vdots & \vdots & \vdots & \vdots & \vdots & \vdots & \vdots & \vdots & \vdots & \vdots & \vdots & \vdots & \vdots & \vdots & \vdots \\
A^{0n*} & 0 & \dots & 0 & 0 & \dots & 0 & \dots & 0 & \dots & 0 & \dots & 0 & 0 & 0 \\
0 & 0 & \dots & 0 & 0 & \dots & 0 & \dots & 0 & \dots & 0 & \dots & 0 & 0 & 0 \\
\vdots & \vdots & \vdots & \vdots & \vdots & \vdots & \vdots & \vdots & \vdots & \vdots & \vdots & \vdots & \vdots & \vdots & \vdots \\
A^{1n*} & 0 & \dots & 0 & 0 & \dots & 0 & \dots & 0 & \dots & 0 & \dots & 0 & 0 & 0 \\
\vdots & \vdots & \vdots & \vdots & \vdots & \vdots & \vdots & \vdots & \vdots & \vdots & \vdots & \vdots & \vdots & \vdots & \vdots \\
0 & 0 & \dots & 0 & 0 & \dots & 0 & \dots & 0 & \dots & A^{(i-1)n} & \dots & 0 & 0 & 0 \\
\vdots & \vdots & \vdots & \vdots & \vdots & \vdots & \vdots & \vdots & \vdots & \vdots & \vdots & \vdots & \vdots & \vdots & \vdots \\
A^{in*} & 0 & \dots & 0 & 0 & \dots & 0 & \dots & 0 & \dots & 0 & \dots & 0 & 0 & 0 \\
\vdots & \vdots & \vdots & \vdots & \vdots & \vdots & \vdots & \vdots & \vdots & \vdots & \vdots & \vdots & \vdots & \vdots & \vdots \\
0 & 0 & \dots & 0 & 0 & \dots & 0 & \dots & 0 & \dots & 0 & \dots & 0 & 0 & A^{(n-2)(n-1)n} \\
A^{(n-2)n*} & 0 & \dots & 0 & 0 & \dots & 0 & \dots & 0 & \dots & 0 & \dots & 0 & 0 & 0 \\
A^{(n-1)n*} & 0 & \dots & 0 & 0 & \dots & 0 & \dots & 0 & \dots & 0 & \dots & 0 & 0 & 0
\end{bmatrix}$$

Figure 3. Matrix **A** from eq 24.

The previously mentioned constraint sets 1 and 2 then lead to the matrix equation: where **A** is a matrix of mixing ratios (shown in Figure 3) and **F** is given as:

$$\mathbf{AF} = \mathbf{F} \quad (24)$$

$$\mathbf{F} = \begin{bmatrix} F^* & F^{01} \dots F^{0n} & F^{12} \dots F^{1n} \dots F^{i(i+1)} & F^{(n-2)n} & F^{(n-1)n} \\ & & \dots F^{in} \dots F^{(n-2)(n-1)} & & \end{bmatrix}^{\mathrm{T}} \quad (25)$$

The sub-matrices A^{ijk} in **A** contain some combination of mixing ratios and zeros. The matrices $\mathbf{A}^{*01}$, $\mathbf{A}^{*02}$, ..., $\mathbf{A}^{*0n}$ contain only ones (see eq 21).

Equation 24 ($\mathbf{AF} = \mathbf{F}$) must be satisfied for any feasible solution to the new finite problem, under the condition that U is large enough that at least one feasible solution exists. Assuming that the units in each set G^{ij} can be rearranged in the proper manner, the column sums of this matrix must satisfy eqs 18, 19, and 21 for the mixing ratios to be feasible for the problem. Because these mixing ratios are between 0 and 1 inclusive, the matrix **A** is a non-negative square matrix with column sum of 1. Bapat and Raghavan[77] have shown that this result proves that the spectral radius of **A** is also 1, using the Perron−Frobenius Theorem (Lemma 3.1.1). This implies that there exists an eigenvector of the matrix **A** that is ≥ 0 and with a corresponding eigenvalue of 1 (see theorem 1.7.3 in the work of Bapat and Raghavan[77]). Therefore, if a matrix **A** of mixing ratios can be found that is feasible for the original optimization problem, one can *always* find a vector F of feasible flows such that $\mathbf{AF} = \mathbf{F}$ and $\mathbf{F} \geq 0$. Using this result, the necessary conditions for a point to be in the feasible set of the transformed problem can be modified, with constraint sets 1, 2, and part of set 7 eliminated, leaving

3. $1 = \sum_{i=0}^{n-1} \sum_{l \in S^{in}} a_{*l}^{in*}$

4. $\bar{C}_* = \sum_{i=0}^{n-1} \sum_{l \in S^{in}} C_l^{in} a_{*l}^{in*}$

5. $1 = \sum_{\substack{i=0 \\ i<j<k}}^{n-2} \sum_{l \in S^{ij}} a_{ml}^{ijk}$

$$\forall m \in S^{jk};\ \forall j = 1, ..., n-1;\ \forall k = 2, ..., n\ (j < k)$$

6. $$\bar{C}_m^{jk} = \sum_{\substack{i=0 \\ i<j<k}}^{n-2} \sum_{l \in S^{ij}} C_l^{ij} a_{ml}^{ijk}$$
$$\forall m \in S^{jk}; \forall j = 1, ..., n-1; \forall k = 2, ..., n \ (j < k)$$

7. $$0 \le a_{lm}^{ijk} \le 1$$
$$\forall m \in S^{ij}; \forall l \in S^{jk}; \forall i = 0, ..., n-2; \forall j = 1, ..., n-1; \forall k = 2, ..., n \ (i < j < k)$$

$$0 \le a_{*l}^{in}* \le 1$$
$$\forall i = 0, ..., n-1; \forall k = 1, ..., n; \forall m \in S^{0k}; \forall l \in S^{in}$$

Constraint 4 can be thought of as a specification on the outlet concentration for the feasible solution. The set of mixing ratios that satisfy the aforementioned constraints defines the AR for the batch reactor network for a given n; this feasible set is similar to that obtained in Manousiouthakis et al.[1] for steady-state RNS. Because of the fact that there is only one network inlet, there can only be one possible inlet concentration set for each reactor/holding tank that is fed at time t_0 (the feed concentration). Similarly, all reactors fed at time t_1 can only be fed by the effluent of the reactor with inlet time t_0 and outlet time t_1 or the holding tank with inlet time t_0 and outlet time t_1. Reactors that feed at time t_2 can be fed by some linear combination of the effluents of reactors/holding tanks that outlet at t_2 and so on. Generally, to ensure causality, a reactor or holding tank that feeds at t_i can be fed only by the linear combination (mixing) of effluents of reactors that outlet at t_i. The fact that the lower triangle (excluding the first column) of matrix **A** (Figure 3) is zero is a manifestation of the network's causality, namely that unit feeds at time t_i can only be comprised of unit effluents at time t_i.

Shrink-Wrap BAR Construction Algorithm

An algorithm that is computationally similar to the "Shrink-Wrap" algorithm (outlined in Manousiouthakis et al.[1]) can be applied to the construction of a superset of the true BAR. Because of the causal nature of the batch RNS problem, this method can only be guaranteed to find a superset to the true BAR. One of the steady-state RNS problem characteristics that leads to the Shrink-Wrap steady-state AR construction method is that any unit's feed can be constructed, through mixing, as a linear combination of the feed and reactor unit exits that belong to the candidate steady-state AR. This was due to the fact that all points in the candidate AR could be constructed independently of each other (through mixing) without consideration of "when" each point was generated. Because unit outlets in the batch reactor network case cannot be used arbitrarily to reconstruct other unit inlets (because of causality), the availability of any arbitrary unit exit in the candidate BAR to mix and convexify the candidate BAR cannot be guaranteed unless one knows when that unit operates. However, a Shrink-Wrap-like algorithm can be used to identify increasingly accurate approximations of a convex set that is guaranteed to contain the BAR for all network operating times n, although it is not guaranteed to necessarily converge to the true BAR. This algorithm removes extreme points (vertices) from an initial superset by following the batch reactor trajectory backward (for a given time, $t_1 - t_0$) and evaluating from where it started. If the starting point of the vertex's trajectory is not a point in the interior of the superset, then no batch reactor can exist that creates that point and the vertex is removed. The algorithm then updates the set as points are removed. The method essentially eliminates points in concentration space (identifying them as "unattainable") by explicitly calculating from where each point must have come. An explicit description of this algorithm is given as follows:

(1) Identify a suitable superset in concentration space for the system in question, based on knowledge of its physical constraints.

(2) Discretize the superset in all directions; the level of accuracy of the method is improved as this discretization becomes finer.

(3) Start from an extreme point of the current set and travel backward along the path of the batch reactor in concentration space from t_1 to t_0. If this new point is in the current set, keep it. If it is not, remove it from the set.

(4) Repeat step 3 until no more extreme points can be removed; this region is guaranteed to contain the true BAR for all network operating times n and for a given reaction/holding time, $t_1 - t_0$.

Breadth-First BAR Construction Algorithm

The aforementioned Shrink-Wrap-like algorithm is only guaranteed to converge to a superset of the BAR. An alternative algorithm that is guaranteed to converge to BAR_n (for any given n) is given next. BAR_n is "grown" from time t_0 out to time t_n, to respect the time hierarchy of the unit operations in a forward dynamic programming-like manner.[6] The algorithm is an instance of a breadth-first search (see the work of Cormen et al.[78]) with the network feed as the first point in concentration space in the candidate BAR. At each stage of generation, the points or nodes form a directed acyclic graph (DAG). Because of this, it is easy to construct an actual network of operations from the nodes of the graph. Each node of the DAG, other than the first, can either have a single parent or multiple parents, because of mixing. If the node is generated by a batch reactor simulation, it has only one parent and that batch reactor operation will be added to the resulting network of reactors to create that node. If the node is generated by a linear combination of other nodes (mixing), it will have two or more parents. At least one of the parent nodes is a newly generated vertex from the previous time step, because we have assumed that mixing is instantaneous. An outline of the algorithm is given as follows:

(1) Start from the feed point—this is the BAR at time t_0 or BAR_0.

(2) Travel along the path of the batch reactor in concentration space from t_0 to t_1. This will be the exit concentration vector of the first batch reactor.

(3) Find the convex hull of all the points from the previous time step and the points from the new time step to find the BAR at that particular time. For the first time step, this will be a line. This is BAR_1.

(4) Discretize this line and travel from time t_1 to time t_2 along the reactor trajectories starting at all discretized points on the line BAR_1 that are not part of BAR_0.

(5) Form the convex hull of this new set and BAR_1; this is an approximation of BAR_2.

(6) For every BAR_i, (a) generate the reactor trajectories from time t_i to time t_{i+1} for all points of BAR_i on an appropriately defined grid that are not contained in BAR_{i-1}, and (b) form the convex hull of this new set of points with the approximation of BAR_i (this is an approximation of BAR_{i+1}).

(7) Repeat step 6 until time t_n; this final convex hull is an approximation of BAR_n, the true BAR at t_n.

Table 2. List of Points Used in Forming BAR_0, BAR_1, BAR_2, BAR_3, and BAR

point	first generated in	C(A)	C(C)	formed by
A	BAR_2	0.2486	0.3204	mixing
B	BAR_2	0.1667	0.3493	map of point C
C	BAR_1	0.375	0.2466	map of point F
D	BAR_3	0.0625	0.3931	map of point B
E	BAR_3	0.2158	0.3495	mixing
F	BAR_0	1.0	0.0	network feed point
G	BAR_3	0.1064	0.3882	map of point A
H	BAR	0.0	0.1851	see Appendix C
W	BAR	0.05752	0.4568	map of point Z
Y	BAR	0.0	0.4666	see Appendix D
Z	BAR	0.1579	0.4156	see Appendix D

Case Study for Trambouze Kinetics

We will apply the two aforementioned algorithms to the construction of the BAR for a case study that exhibits Trambouze[79] reaction kinetics (example 4 from his 1959 work), which is a reaction scheme that is often studied in the literature:[1,38,55]

$$A \xrightarrow{k_1} B \text{ (zeroth order, } k_1 = 0.025 \text{ mol L}^{-1} \text{ min}^{-1}) \quad (26)$$

$$A \xrightarrow{k_2} C \text{ (first order, } k_2 = 0.2 \text{ min}^{-1}) \quad (27)$$

$$A \xrightarrow{k_3} D \text{ (second order, } k_3 = 0.4 \text{ L mol}^{-1} \text{ min}^{-1}) \quad (28)$$

These are the same reaction kinetics and parameters as those given in the work of Manousiouthakis et al.[1] The rates of generation for each species for this reaction pathway are

$$R_A = -k_1 - k_2 C_A - k_3 C_A^2 \quad (29)$$

$$R_B = k_1 \quad (30)$$

$$R_C = k_2 C_A \quad (31)$$

$$R_D = k_3 C_A^2 \quad (32)$$

The batch reactor equations can be solved analytically, as described in Appendix A. This makes this example ideal for testing our candidate BAR_n identification algorithms, because they can be compared analytically to the true BAR_n at each time. For the purpose of creating BAR_ns for this example, we consider that the batch reactor time is 2 min, i.e., that $\tau = t_n - t_{n-1} = t_{n-1} - t_{n-2} = \ldots = t_1 - t_0 = 2$ min.

For this batch reactor time, BAR_0, BAR_1, BAR_2, and BAR_3 are created analytically for this example as described by Appendix B and BAR (BAR_n as $n \rightarrow \infty$) is identified as described by Appendices C and D. A table of points that define these regions is given as Table 2. Table 3 lists the points and curves that define BAR_0, BAR_1, BAR_2, BAR_3, and BAR, for easy reference.

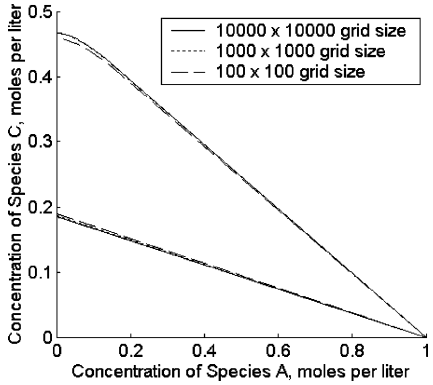

Figure 4. Shrink-Wrap-like algorithm superset for $t_{in} - t_{out} = 2$ min and varying grid size.

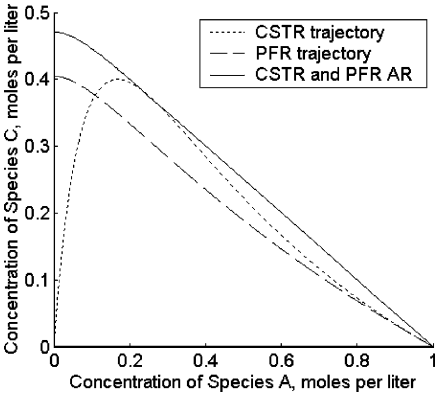

Figure 5. Attainable region (AR) for steady-state networks.

Shrink-Wrap BAR Construction Algorithm Results for the Trambouze Example

Figure 4 shows increasingly accurate approximations of a superset to the BAR for species A (x-axis) and species C (y-axis), ranging from a 100 × 100 grid size to a 10 000 × 10 000 grid size. The identified BAR superset is only slightly smaller than the steady-state AR found in the work of Manousiouthakis et al.[1] (shown in Figure 5) at the high end of the y-axis intersection of the AR (0.4666 for BAR, versus 0.4705 for steady-state AR), but significantly smaller at the lower end of

Table 3. List of Points and Relevant Equations for Curves That Define BAR_0, BAR_1, BAR_2, BAR_3, and BAR

region	defined by	relevant equations
BAR_0	point F	$F = (1.0,0.0)$
BAR_1	points C to F (line f_1)	$f_1(C_1(A)) = C_1(C) = 0.8(0.2 - \ln 2)(C_1(A) - 1)$
BAR_2	points A to B (g_1), B to C (line), C to F (line), and F to A (line)	$g_1(C_2(A)) = C_2(C) = (0.2 - \ln 2)\dfrac{8C_2(A) - 3}{4 - 4C_2(A)} + \ln\left(\sqrt{\dfrac{5}{4 - 4C_2(A)}}\right) - 0.1$
BAR_3	points E to G (h_1), G to D (h_2), D to C (line), C to F (line), F to E (line)	$h_1(C_3(A)) = C_3(C) = 0.4264\left(\dfrac{15 - 40C_3(A)}{16 - 16C_3(A)}\right) + \ln\left(\sqrt{\dfrac{5}{4 - 4C_3(A)}}\right) - 0.1$
		$h_2(C_3(A)) = C_3(C) = (0.2 - \ln 2)\dfrac{12C_3(A) - 2}{3 - 8C_3(A)} + \ln\left(\sqrt{\dfrac{5}{3 - 8C_3(A)}}\right) - 0.2$
BAR	points Z to W (j_1), W to Y (j_2), Y to H (line), H to F (line), F to Z (line)	$j_1(C(A)) = C(C) = \left(\dfrac{40C(A) - 15}{16 - 16C(A)}\right)\dfrac{C_Z(C)}{C_Z(A) - 1} + 0.5\ln\left(\dfrac{5}{4 - 4C(A)}\right) - 0.1$
		$j_2(C(A)) = C(C) = \left(\dfrac{30C(A) - 5}{6 - 16C(A)}\right)\dfrac{C_Z(C)}{C_Z(A) - 1} + 0.5\ln\left(\dfrac{5}{3 - 8C(A)}\right) - 0.2$

the *y*-axis intersection of the AR (0.1851 for BAR, versus 0.0 for steady-state AR). Fundamentally, the reason for this discrepancy is the causality restriction that has been imposed on the batch network; the point (0.0, 0.0) cannot be part of the BAR because no batch reactor trajectory with a feed in BAR can have this point as an exit. Similarly, the point (0.0, 0.1) cannot be part of BAR for the same reason. Repeated application of this argument within the aforementioned Shrink-Wrap-like algorithm leads to the lower boundary of the BAR superset being the line that goes through the network feed point (1.0, 0.0), a batch reactor exit that lies on the *y*-axis, and its corresponding feed. Solving the batch reactor equations in Appendix A for a reaction time of 2 min and an outlet concentration of A of 0.0 mol/L gives an inlet concentration of A of 0.0625 or $^1/_{16}$ mol/L. Also using Appendix A, a batch reactor that feeds at (0.0625, $\bar{C}$(C)) will exit at (0, $\bar{C}$(C) + 0.01157). The value of $\bar{C}$(C) for which the network feed point, aforementioned reactor inlet, and reactor outlet points are all on the same line is:

$$\frac{\bar{C}(\mathrm{C})}{0.0625-1}=\frac{\bar{C}(\mathrm{C})+0.01157}{-1}\Rightarrow$$

$$\bar{C}(\mathrm{C})=15(0.01157)=0.1736$$

Thus, the batch reactor exit is:

$$C(\mathrm{C})=0.01157=16(0.01157)=0.1851$$

This is consistent with the Shrink-Wrap-like BAR code, which identifies the lowest concentration attainable on the C(C) axis as point H (0.0, 0.1851).

The BAR superset identified in Figure 4 is, in fact, the BAR itself. As discussed in detail in Appendix C, if the point of BAR_3 with the lowest value of C(A) is considered to be a batch reactor feed point, then this batch reactor's exit is on the *y*-axis. Mixing this exit with the network feed results in a point with $C(\mathrm{A}) = 0.0625$ that is below the point in BAR_3 with the same value of C(A). Repeated application of this batch reaction/mixing process is shown in Appendix C to reach the lower boundary of the previously identified BAR superset. A similar procedure is outlined in Appendix D for the upper boundary of the superset, thus establishing that the superset given in Figure 4 is the actual BAR.

These results suggest that if species C were an unwanted byproduct of this reaction set, choosing any network of batch reactors with a reaction/holding time of 2.0 min would give unacceptable results; a network of steady-state reactors (e.g., a CSTR) could yield practically no generation of C and, thus, would be superior to a network of batch reactors (except when the reaction/holding time becomes very, very small.)

Breadth-First BAR Construction Algorithm Results for the Trambouze Example

A "breadth-first" algorithm can be used to identify the BAR_n for any given n; we show the case for $n = 3$ as depicted in Figure 6 and an enlargement of the top of the same region as Figure 7 to illustrate the convergence of the algorithm with an increasing number of grid points.

This result matches very well with the analytical calculation of BAR_3 that is given in Appendix B.

Conclusions

We have outlined a method for automatically identifying the attainable region for batch reactor networks for a given overall network time, for any number of components, and for any isothermal kinetic model. We have shown that a batch reactor model can be incorporated into the IDEAS framework, which is proven to identify the globally optimal network of batch reactors.

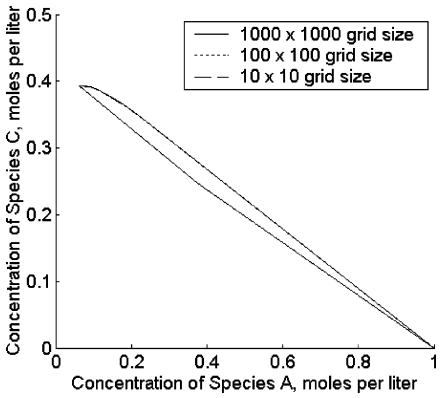

Figure 6. Breadth-first algorithm results for BAR_3 with $t_{in} - t_{out} = 2$ min and varying grid size.

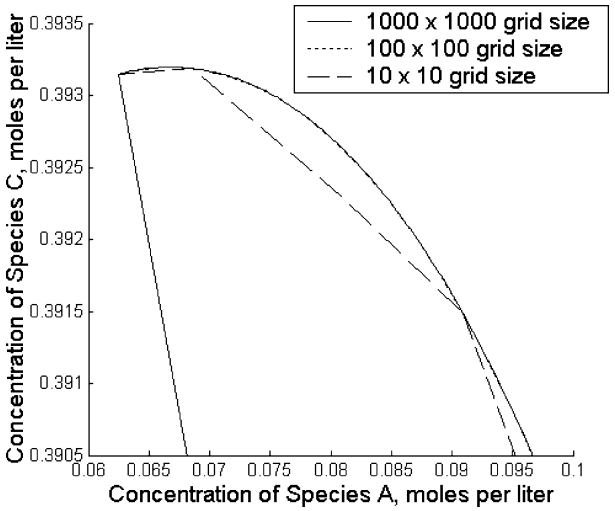

Figure 7. Enlargement of Figure 6.

We have demonstrated that a Shrink-Wrap-like algorithm can be used to identify increasingly accurate approximations of a superset of the batch attainable region (BAR). We have also outlined a novel breadth-first algorithm that can be used to identify the batch reactor network BAR_n. We have applied both algorithms to a case study with Trambouze kinetics, and we have demonstrated that the breadth-first algorithm accurately identifies BAR_n (for $n = 3$), whereas the Shrink-Wrap-like algorithm accurately identifies not only a superset of BAR but the actual BAR itself. Iterative procedures that demonstrate how the BAR boundary, as identified by the Shrink-Wrap-like algorithm, can be reached with causal (forward moving in time) batch reaction and mixing operations are discussed in detail.

Appendix A: Solution of Batch Reactor Model for Trambouze Kinetics

The considered Trambouze kinetics ($k_1 = 0.025$, $k_2 = 0.2$, $k_3 = 0.4$) satisfy the relation $(k_2^2 - 4k_1k_3)^{1/2} = 0$. Therefore, any batch reactor trajectory satisfies the following relations:

$$C(\mathrm{A})=\frac{(2-k_2\tau)\bar{C}(\mathrm{A})-\alpha k_2\tau}{2k_3\tau\bar{C}(\mathrm{A})+2+k_2\tau}$$

$$C(\mathrm{C})=\bar{C}(\mathrm{C})+\alpha[2\ln(1+\alpha k_3\tau+k_3\tau\bar{C}(\mathrm{A}))-k_2\tau]$$

where τ is the reaction time of unit, α is defined as:

$$\alpha \equiv \frac{k_2}{2k_3} = \frac{1}{4}$$

$\bar{C}(A)$ and $C(A)$ respectively represent the inlet and outlet concentrations of species A, and $\bar{C}(C)$ and $C(C)$ respectively represent the inlet and outlet concentrations of species C.

For $\tau = 2.0$:

$$C(A) = \frac{\bar{C}(A) - 0.0625}{\bar{C}(A) + 1.5} \Rightarrow \bar{C}(A) = \frac{1 + 24C(A)}{16 - 16C(A)}$$

and:

$$C(C) = 0.5 \ln(0.8\bar{C}(A) + 1.2) - 0.1$$

Appendix B: Analytical Generation of BAR_0, BAR_1, BAR_2, and BAR_3

BAR_0 consists solely of the feed point: $BAR_0 = \{(1.0,0)\} = \{(\bar{C}_0(A),\bar{C}_0(C))\}$.

BAR_1 is the convex hull (which, in this case, is a line) between two points: the feed and the exit of a batch reactor with $\tau = 2.0$ and with the feed point as its inlet. Based on the formulas given previously, the latter point is $(C_0(A), C_0(C)) = (0.375, \ln(\sqrt{2}) - 0.1)$. We will call this point C. BAR_1 can be defined as

$$BAR_1 = \{(C_1(A), C_1(C))$$

where:

$$C_1(C) = f_1(C_1(A))$$

$$C_1(A) \in [0.375, 1.0]\}$$

and:

$$f_1(C_1(A)) \equiv 0.8(0.2 - \ln 2)(C_1(A) - 1)$$

BAR_2 is the convex hull of all batch reactor trajectories starting from points in BAR_1 and BAR_1. It can be defined as follows:

$$C_2(A) = \frac{C_1(A) - 0.0625}{C_1(A) + 1.5} = f_2(C_1(A)) \Rightarrow$$

$$C_2(A) \in [0.1667, 0.375]$$

$$C_2(C) = C_1(C) + 0.5 \ln(0.8C_1(A) + 1.2) - 0.1 =$$
$$0.8(0.2 - \ln 2)(C_1(A) - 1) + 0.5 \ln(0.8C_1(A) + 1.2) -$$
$$0.1 = f_3(C_1(A))$$

The convexification of this region will be a line from one endpoint of the BAR_1 line to either another endpoint of the new set, or a point intermediate on that new set, depending on whether the new set has an inflection point in the domain:

$$C_2(C) = (0.2 - \ln 2)\left(\frac{8C_2(A) - 3}{4 - 4C_2(A)}\right) +$$
$$0.5 \ln\left(\frac{5}{4 - 4C_2(A)}\right) - 0.1 \equiv g_1(C_2(A))$$

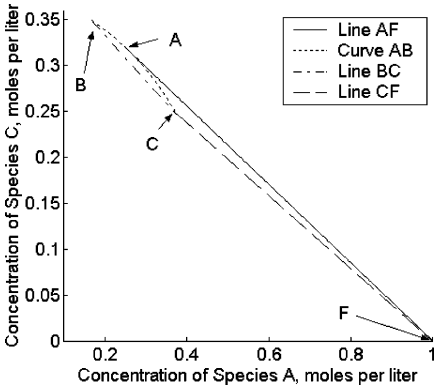

Figure B1. BAR_2 generated analytically.

where:

$$g_1\left(\frac{3}{8}\right) = \ln(\sqrt{2}) - 0.1 = 0.2466$$

$$g_1\left(\frac{1}{6}\right) = \ln(\sqrt{3}) - 0.2 = 0.3493$$

Thus:

$$C_2(C) \in [0.2466, 0.3493]$$

We must determine if there is a point in the domain of g_1 whose tangent intersects the feed point:

$$\frac{g_1(C_2(A)) - 0}{C_2(A) - 1} = \frac{dg_1(C_2(A))}{dC_2(A)} \Rightarrow \ln\left(\frac{5}{4 - 4C_2(A)}\right) =$$
$$\frac{1 - (\ln 2) - 4(\ln 2)C_2(A)}{C_2(A) - 1} \Rightarrow C_2(A) = 0.2486$$

$$g_1(0.2486) = \left(\frac{1.6(0.2486) + 5(\ln 2) - 2.6}{4 - 4(0.2486)}\right) -$$
$$0.1 = 0.3204$$

This result shows that such a point exists; we will call this point (0.2486, 0.3204) point A. The function g_1 is concave on the domain; therefore, BAR_2 is the area formed by the line from the feed point to point A, the part of the batch reactor trajectory from point A to point B ($^1/_6$, $0.5(\ln 3) - 0.2$), the line from point B to point C ($^3/_8$, $0.5(\ln 2) - 0.1$), and the line from point C to the feed point (see Figure B1).

BAR_3 for this problem is comprised of all points attainable from batch reactor trajectories that start on the boundary of BAR_2. We only need to consider extreme points, because the Trambouze reaction vector is dependent only on the concentration of species A; any reactor inlet point on a given vertical line that satisfies the relation:

$$\bar{C}^l(C) \le \bar{C}(C) \le \bar{C}^u(C)$$

will be mapped to a point $(C(A), C(C))$ that lies between the points $(C(A), C^l(C))$ and $(C(A), C^u(C))$. Therefore one must only consider the reactor trajectory that extends the region the furthest for each point on the $C(A)$ axis. Three separate segments need to be mapped (i.e., travel along the batch reactor trajectories for 2 min) to create BAR_3: line AF, curve AB, and line BC. Line CF does not need to be mapped again, because its map was calculated previously and has already been considered in BAR_2. The convex hull of the region that is defined by these

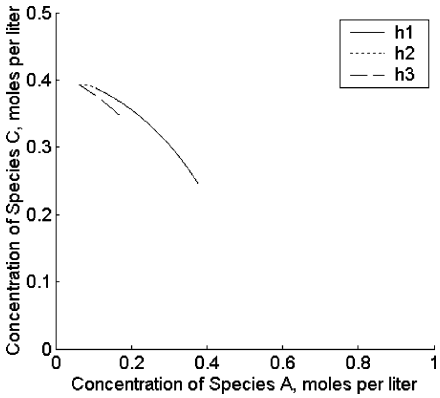

Figure B2. New mappings needed to make BAR_3.

three mappings and BAR_2 will give BAR_3. Mapping line AF gives:

$$C_3(\mathrm{C}) = 0.4264\left(\frac{15 - 40C_3(\mathrm{A})}{16 - 16C_\mathrm{C}(\mathrm{A})}\right) + 0.5\ln\left(\frac{5}{4 - 4C_3(A)}\right) - 0.1 \equiv h_1(C_3(\mathrm{A})), \qquad C_3(\mathrm{A}) \in [0.1064, 0.375]$$

Mapping curve AB gives

$$C_3(\mathrm{C}) = \frac{(12C_3(\mathrm{A}) - 2)(0.2 - \ln 2)}{3 - 8C_3(\mathrm{A})} + \ln\sqrt{\frac{5}{3 - 8C_3(\mathrm{A})}} - 0.2 \equiv h_2(C_3(\mathrm{A})), \qquad C_3(\mathrm{A}) \in [0.0625, 0.1064]$$

Mapping line BC gives

$$C_3(\mathrm{C}) = 2.4\left(\ln\left(\frac{2}{3}\right) + 0.2\right)\left(\frac{1 + 24C_3(\mathrm{A})}{16 - 16C_3(\mathrm{A})}\right) + 0.5\ln\left(\frac{5}{4 - 4C_3(A)}\right) + 0.9(\ln 3) - 0.4(\ln 2) - 0.38 \equiv h_3(C_3(\mathrm{A})), \qquad C_3(\mathrm{A}) \in [0.0625, 0.1667]$$

A plot of these three mappings is given as Figure B2.

To form BAR_3, we must make the convex hull of these new points with the points of BAR_2. We first determine if h_1 has a tangent that intersects the feed point:

$$\frac{h_1(C_3(\mathrm{A})) - 0}{C_3(\mathrm{A}) - 1} = \frac{\mathrm{d}h_1(C_3(\mathrm{A}))}{\mathrm{d}C_3(\mathrm{A})}, \qquad C_3(\mathrm{A}) = 0.2158 \in [0.1064, 0.375] \Longrightarrow$$

$$-0.4264\left(\frac{15}{8} - 5C_3(\mathrm{A})\right) + 0.8C_3(\mathrm{A}) + 0.5325 = [1 - C_3(\mathrm{A})]\ln\left(\frac{5}{4 - 4C_3(\mathrm{A})}\right)$$

We see that h_1 does, in fact, intersect the feed point and is concave, so there will be a convexification line from the feed point to point E (0.2158, 0.3495). Because h_2 is also concave and its derivative is equal to the derivative of h_1 at their intersection, there will be no further convexifications at the top of the region. The function h_3 is concave and the value of C_3(C) for h_3 at point B is greater than that of line CD at the C_3(A) of point B; therefore, there is a convexification line from point C to point D (0.0625, 0.393147) to finish BAR_3. This completes the analytical generation of BAR_3; it is the region formed by the line from the feed to point E on h_1, the function h_1 from point E to point G (0.1064, 0.3882), the function h_2 from point G to point D, the line from point D to point C, and line CF (previously defined). The final graph of BAR_3 appears almost identical to the result from the breadth-first algorithm (Figure 6) and will not be reproduced.

Appendix C: Analytical Generation of the Bottom of BAR

The point in BAR_3 with the lowest value of C(A) is (0.0625, 0.3931). This point maps to the point (0, 0.4047). The equation for the line from this point to the feed point is C(C) = 0.4047-(1 − C(A)). The point on this new line at C(A) = 0.0625 is C(C) = 0.3794. Mapping this new point back to the axis gives the point (0, 0.3910). This procedure can be repeated iteratively as follows; define C_i(C) as the ith C(C) value in the sequence and ΔC(C) as the increase gained by mapping, where C_0(C) = 0.3931 and ΔC(C) = 0.01157. The first three points in the sequence are then:

$$C_1(\mathrm{C}) = \left(\frac{15}{16}\right)[C_0(\mathrm{C}) + \Delta C(\mathrm{C})]$$

$$C_2(\mathrm{C}) = \left(\frac{15}{16}\right)^2 C_0(\mathrm{C}) + \left[\left(\frac{15}{16}\right) + 1\right]\left(\frac{15}{16}\right)\Delta C(\mathrm{C})$$

$$C_3(\mathrm{C}) = \left(\frac{15}{16}\right)^3 C_0(\mathrm{C}) + \left[\left(\frac{15}{16}\right)^2 + \left(\frac{15}{16}\right) + 1\right]\left(\frac{15}{16}\right)\Delta C(\mathrm{C})$$

and C_n(C), in the limit as $n \to \infty$, can be expressed as:

$$\lim_{n\to\infty} C_n(\mathrm{C}) = C_0(\mathrm{C}) \lim_{n\to\infty}\left(\frac{15}{16}\right)^n + \left(\frac{15}{16}\right)\Delta C(\mathrm{C}) \lim_{n\to\infty}\sum_{i=0}^{n}\left(\frac{15}{16}\right)^i = 15\Delta C(\mathrm{C}) = 0.1736$$

This point maps forward along a reactor trajectory for 2.0 min to point H (0, 0.1851), which is also the lowest point on the C(C) axis obtained through the Shrink-Wrap-like algorithm.

Appendix D: Analytical Generation of the Top of BAR

As shown in the construction of BAR_2 and BAR_3, at high values of C(A) (C(A) > 0.375), the upper BAR_n boundary is a straight line that is tangent to the curve generated when each point of the upper BAR_{n-1} boundary (which, again, is a straight line for large values of C(A)) is considered a feed to a batch reactor with a reaction time of τ = 2.0 min. BAR_2 has, as its upper boundary, the line AF, which is tangent to the curve CAB (at point A), which is generated when the points of the upper boundary of BAR_1 (line CF) are considered as feeds to batch reactors with τ = 2.0. Similarly, BAR_3 has, as its upper boundary, the line EF, which is tangent (at point E) to the curve $h_1(C_3(\mathrm{A}))$. This curve consists of points that are outlets of batch reactors that have, as feeds, the points on the upper boundary of BAR_2 (line AF). This process will stop expanding BAR_i upward (as $i \to \infty$) only when the line ZF (that is, the upper boundary of BAR_i) is tangent at point Z to the curve that results from mapping the line ZF through the batch reactor map with τ = 2.0. To identify this point Z (Z = (C_Z(A), C_Z(C)), the following conditions must hold:

(1) All points on the line ZF satisfy:

$$\frac{\bar{C}(\mathrm{C})}{\bar{C}(\mathrm{A}) - 1} = \frac{C_\mathrm{Z}(\mathrm{C})}{C_\mathrm{Z}(\mathrm{A}) - 1}$$

(2) The line ZF maps to the following curve:

$$C(\mathrm{C}) = \left(\frac{40C(\mathrm{A}) - 15}{16 - 16C(\mathrm{A})}\right)\frac{C_Z(\mathrm{C})}{C_Z(\mathrm{A}) - 1} + 0.5\ln\left(\frac{5}{4 - 4C(\mathrm{A})}\right) - 0.1 \equiv j_1(C(\mathrm{A}))$$

(3) At $C(\mathrm{A}) = C_Z(\mathrm{A})$, $C(\mathrm{C}) = C_Z(\mathrm{C})$ and $\mathrm{d}C(\mathrm{C})/\mathrm{d}C(\mathrm{A})$ is given as:

$$\frac{\mathrm{d}C(\mathrm{C})}{\mathrm{d}C(\mathrm{A})} = \frac{C_Z(\mathrm{C})}{C_Z(\mathrm{A}) - 1}$$

where:

$$C_Z(\mathrm{C}) = \frac{8(1 - C_Z(\mathrm{A}))^2}{25 - 16(1 - C_Z(\mathrm{A}))^2}$$

Taking the derivative of the function j_1 from condition 2 above and evaluating the derivative at $C_Z(\mathrm{A})$ yields:

$$\left.\frac{\mathrm{d}j_1(C(\mathrm{A}))}{\mathrm{d}C(\mathrm{A})}\right|_{C(\mathrm{A})=C_Z(\mathrm{A})} = \frac{0.5(C_Z(\mathrm{A}))^2 - C_Z(\mathrm{A}) - \left(\frac{25}{16}\right)C_Z(C) + 0.5}{(1 - C_Z(\mathrm{A}))^3}$$

This point must be on the map of line ZF (condition 2), giving the coordinates of point Z, $(C_Z(\mathrm{A}),C_Z(\mathrm{C})) = (0.1579, 0.4156)$. Because, by definition, line ZF and its map have the same slope at point Z, there is no need to convexify the top of the BAR near point Z. Next, we define point W (0.05752, 0.4568) as the point to which point Z maps after a batch reaction time of 2.0 min; the portion of the mapping of line ZF between point Z and point W will now be called curve ZW, as defined by the function j_1. The second derivative of j_1, with respect to $C(\mathrm{A})$, is negative between point Z and point W, so the curve ZW is concave between point Z and point W. We can now map curve ZW, through the batch reactor map with $\tau = 2.0$, until it reaches the $C(\mathrm{A})$ axis to complete the top of BAR:

$$C(\mathrm{C}) = \left(\frac{30C(\mathrm{A}) - 5}{6 - 16C(\mathrm{A})}\right)\frac{C_Z(\mathrm{C})}{C_Z(\mathrm{A}) - 1} + 0.5\ln\left(\frac{5}{3 - 8C(\mathrm{A})}\right) - 0.2 \equiv j_2(C(\mathrm{A}))$$

The map hits the $C(\mathrm{A})$ axis at $C(\mathrm{C}) = 0.4666$. We will call this point Y (Y = (0.0, 0.4666)) and refer to the portion of the map of ZW for $\tau = 2.0$ min that remains in the physical region (i.e., $C(\mathrm{A}) \geq 0$) as curve WY. A plot of line ZF, curve ZW, and curve WY is given as Figure D1. The derivatives of curve ZW at point W and curve WY at point W are equal:

$$\left.\frac{\mathrm{d}j_1(C(\mathrm{A}))}{\mathrm{d}C(\mathrm{A})}\right|_{C(\mathrm{A})=C_W(\mathrm{A})} = \frac{4(6C_W(\mathrm{A}) - 1)}{(1 + 4C_W(\mathrm{A}))(7 - 12C_W(\mathrm{A}))} = \left.\frac{\mathrm{d}j_2(C(\mathrm{A}))}{\mathrm{d}C(\mathrm{A})}\right|_{C(\mathrm{A})=C_W(\mathrm{A})}$$

In addition, curve WY is concave between point Y and point W, so no convexification line is necessary to fill in the region; the top of the BAR is the line from the feed point F to point Z, the function j_1 from point Z to point W, and the function j_2 from point W to point Y. This turns out to be approximated extremely well by the Shrink-Wrap-like algorithm, which, in this case, has successfully identified the BAR itself.

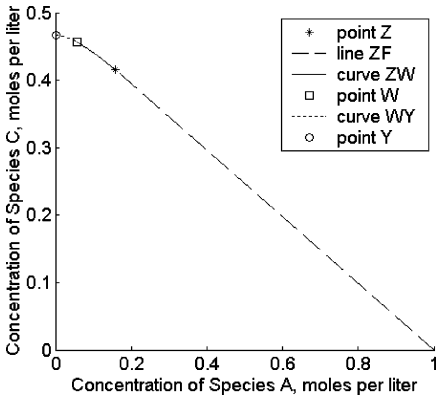

Figure D1. Point Z, line ZF, curve ZW, point W, curve WY, and point Y (complete top of BAR).

Literature Cited

(1) Manousiouthakis, V.; Justanieah, A.; Taylor, L. The Shrink-Wrap Algorithm for the Construction of the Attainable Region: Application of the IDEAS Framework. *Comput. Chem. Eng.* **2004**, *28*, 1563.

(2) Chitra, S.; Govind, R. Yield Optimization for Complex Reaction Systems. *Chem. Eng. Sci.* **1981**, *36*, 1219.

(3) Chitra, S.; Govind, R. Synthesis of Optimal Serial Reactor Structures for Homogeneous Reactions. Part I: Isothermal Reactors. *AIChE J.* **1985**, *31*, 177.

(4) Chitra, S.; Govind, R. Synthesis of Optimal Serial Reactor Structures for Homogeneous Reactions. Part II: Non-Isothermal Reactors. *AIChE J.* **1985**, *31*, 185.

(5) Ong, S. Optimization of CSTRs in Series by Dynamic Programming. *Biotechnol. Bioeng.* **1986**, *28*, 818.

(6) Bellman, R. *Dynamic Programming*; Princeton University Press: Princeton, NJ, 1957.

(7) Pibouleau, L.; Floquet, P.; Domenech, S. Optimal Synthesis of Reactor−Separator Systems by Non-Linear Programming Method. *AIChE J.* **1988**, *34*, 163.

(8) Omtveit, T.; Wah, P.; Lien, K. Decomposed Algorithmic Synthesis of Reactor−Separation−Recycle Systems. *Comput. Chem. Eng.* **1994**, *18*, 1115.

(9) Smith, E.; Pantelides, C. Design of Reaction/Separation Networks Using Detailed Models. *Comput. Chem. Eng.* **1995**, *19*, S83.

(10) Bikic, D.; Glavic, P. Synthesis of Reactor Networks with Multiple Multi-Component Feeds. *Comput. Chem. Eng.* **1995**, *19*, S161.

(11) Bikic, D.; Glavic, P. Innovative Designs of Reactor Networks from Reaction and Mixing Principles. *Comput. Chem. Eng.* **1996**, *20*, S455.

(12) Bikic, D.; Glavic, P. Towards Automatic Generation of Novel Reactor−Separator Networks with Multiple Multi-Component Feeds. *Comput. Chem. Eng.* **1997**, *21*, S41.

(13) Esparta, A.; Obertopp, T.; Gilles, E. Synthesis of Isothermal Fluid−Fluid Two-Phase CSTR Networks. *Comput. Chem. Eng.* **1998**, *22*, S671.

(14) Hua, K.; Li, Y.; Hu, S.; Shen, J. Three-Distribution-Parameter General Model for Reactor Network Synthesis. *Comput. Chem. Eng.* **2000**, *24*, 217.

(15) Mehta, V.; Kokossis, A. Non-Isothermal Synthesis of Homogeneous and Multiphase Reactor Networks. *AIChE J.* **2000**, *46*, 2256.

(16) Pahor, B.; Irsic, N.; Kravanja, Z. MINLP Synthesis and Modified Attainable Region Analysis of Reactor Networks in Overall Process Schemes Using More Compact Reactor Superstructure. *Comput. Chem. Eng.* **2000**, *24*, 1403.

(17) Pahor, B.; Kravanja, Z.; Bedenik, N. Synthesis of Reactor Networks in Overall Process Flowsheets Within the Multilevel MINLP Approach. *Comput. Chem. Eng.* **2001**, *25*, 765.

(18) Grossmann, I. E.; Caballero, J. A.; Yeomans, H. Advances in Mathematical Programming for Automated Design, Integration and Operation of Chemical Processes. In *Proceedings of the International Conference on Process Integration (PI '99)*, Copenhagen, Denmark, 1999

(19) Aris, R. *The Optimal Design of Chemical Reactors*; Academic Press: New York, 1961.

(20) Paynter, J.; Haskins, D. Determination of Optimal Reactor Type. *Chem. Eng. Sci.* **1970**, *25*, 1415.

(21) Waghmare, R. S.; Lim, H. C. Optimal Operation of Isothermal Reactors. *Ind. Eng. Chem. Fundam.* **1981**, *20*, 361.

(22) Parulekar, S. J.; Waghmare, R. S.; Lim, H. C. Yield Optimization for Multiple Reactions. *Chem. Eng. Sci.* **1988**, *43*, 3077.

(23) Achenie, L.; Biegler, L. Algorithmic Synthesis of Chemical Reactor Networks Using Mathematical Programming. *Ind. Eng. Chem. Res.* **1986**, *25*, 621.

(24) Achenie, L.; Biegler, L. Developing Targets for the Performance Index of a Chemical Reactor Network: Isothermal Systems. *Ind. Eng. Chem. Res.* **1988**, *27*, 1811.

(25) Achenie, L.; Biegler, L. A Superstructure Based Approach to Chemical Reactor Network Synthesis. *Comput. Chem. Eng.* **1990**, *14*, 23.

(26) Godorr, S.; Hildebrandt, D.; Glasser, D.; McGregor, C. Choosing Optimal Control Policies Using the Attainable Region Approach. *Ind. Eng. Chem. Res.* **1999**, *38*, 639.

(27) Hillestad, M. A Systematic Generation of Reactor Designs I: Isothermal Conditions. *Comput. Chem. Eng.* **2004**, *28*, 2717.

(28) Hillestad, M. A Systematic Generation of Reactor Designs. II: Non-Isothermal Conditions. *Comput. Chem. Eng.* **2005**, *29*, 1101.

(29) Wilson, S.; Manousiouthakis, V. IDEAS Approach to Process Network Synthesis: Application to Multi-Component MEN. *AIChE J.* **2000**, *46*, 2408.

(30) Drake, J.; Manousiouthakis, V. IDEAS Approach to Process Network Synthesis: Minimum Plate Area for Complex Distillation Networks with Fixed Utility Cost. *Ind. Eng. Chem. Res.* **2002**, *41*, 4984.

(31) Drake, J.; Manousiouthakis, V. IDEAS Approach to Process Network Synthesis: Minimum Utility Cost for Complex Distillation Networks. *Chem. Eng. Sci.* **2002**, *57*, 3095.

(32) Justanieah, A.; Manousiouthakis, V. IDEAS Approach to Separation Network Synthesis: Application to Chromium Recovery Form Wastewater. *Adv. Environ. Res.* **2003**, *7*, 549.

(33) Martin, L.; Manousiouthakis, V. Globally Optimal Power Cycle Synthesis via the Infinite-Dimensional State-Space (IDEAS) Approach Featuring Minimum Area with Fixed Utility. *Chem. Eng. Sci.* **2003**, *58*, 4291.

(34) Holiastos, K.; Manousiouthakis, V. Infinite-Dimensional State-Space (IDEAS) Approach to Globally Optimal Design of Distillation Networks Featuring Heat and Power Integration. *Ind. Eng. Chem. Res.* **2004**, *43*, 7826.

(35) Burri, J.; Manousiouthakis, V. Global Optimization of Reactive Distillation Networks Using IDEAS. *Comput. Chem. Eng.* **2004**, *28*, 2509.

(36) Horn, F. Attainable and Non-Attainable Regions in Chemical Reaction Technique. In *Third European Symposium on Chemical Reaction Engineering*; Pergamon Press: London, 1964.

(37) Gavalas, G. *Nonlinear Differential Equations of Chemically Reacting Systems: Springer Tracts in Natural Philosophy*; Springer: New York, 1968.

(38) Glasser, D.; Hildebrandt, D.; Crowe, C. A Geometric Approach to Steady Flow Reactors: The Attainable Region and Optimization in Concentration Space. *Ind. Eng. Chem. Res.* **1987**, *26*, 1803.

(39) Hildebrandt, D.; Glasser, D.; Crowe, C. Geometry of the Attainable Region Generated by Reaction and Mixing: With and Without Constraints. *Ind. Eng. Chem. Res.* **1990**, *29*, 49.

(40) Glasser, D.; Hildebrandt, D.; Godorr, S. The Attainable Region for Segregated Maximum Mixed and Other Reactor Models. *Ind. Eng. Chem. Res.* **1994**, *33*, 1136.

(41) Hopley, F.; Glasser, D.; Hildebrandt, D. Optimal Reactor Structures for Exothermic Reversible Reactions with Complex Kinetics. *Chem. Eng. Sci.* **1996**, *51*, 2399.

(42) Nicol, W.; Hernier, M.; Hildebrandt, D.; Glasser, D. The Attainable Region and Process Synthesis: Reaction Systems with External Cooling and Heating. *Chem. Eng. Sci.* **2001**, *56*, 173.

(43) Feinberg, M.; Hildebrandt, D. Optimal Reactor Design from a Geometric Viewpoint Part I: Universal Properties of the Attainable Region. *Chem. Eng. Sci.* **1997**, *52*, 1637.

(44) Feinberg, M. Recent Results in Optimal Reactor Synthesis via Attainable Region Theory. *Chem. Eng. Sci.* **1999**, *54*, 2535.

(45) Feinberg, M. Optimal Reactor Design from a Geometric Viewpoint. Part II: Critical Sidestream Reactors. *Chem. Eng. Sci.* **2000**, *55*, 2455.

(46) Feinberg, M. Optimal Reactor Design from a Geometric Viewpoint. Part III: Critical CFSTRs. *Chem. Eng. Sci.* **2000**, *55*, 3553.

(47) McGregor, C.; Glasser, D.; Hildebrandt, D. The Attainable Region and Pontryagin's Maximum Principle. *Ind. Eng. Chem. Res.* **1999**, *38*, 652.

(48) Rooney, W.; Hausberger, B.; Biegler, L.; Glasser, D. Convex Attainable Region Projections for Reactor Network Synthesis. *Comput. Chem. Eng.* **2000**, *24*, 225.

(49) Nisoli, A.; Malone, M.; Doherty, M. Attainable Regions for Reaction with Separation. *AIChE J.* **1997**, *43*, 374.

(50) Smith, R.; Malone, M. Attainable Regions for Polymerization Reaction Systems. *Ind. Eng. Chem. Res.* **1997**, *36*, 1076.

(51) Gadewar, S.; Malone, M.; Doherty, M. Feasible Region for a Counter-Current Cascade of Vapor−Liquid CSTRs. *AIChE J.* **2002**, *48*, 800.

(52) Kauchali, S.; Hausberger, B.; Hildebrandt, D.; Glasser, D.; Biegler, L. Automating Reactor Network Synthesis: Finding a Candidate Attainable Region for the Water-Gas Shift (WGS) Reaction. *Comput. Chem. Eng.* **2004**, *28*, 149.

(53) Omtveit, T.; Tanskanen, J.; Lien, K. Graphical Targeting Procedures for Reactor Systems. *Comput. Chem. Eng.* **1994**, *18*, S113.

(54) Burri, J.; Wilson, S.; Manousiouthakis, V. Infinite Dimensional State-Space Approach to Reactor Network Synthesis: Application to Attainable Region Construction. *Comput. Chem. Eng.* **2002**, *26*, 849.

(55) Kauchali, S.; Rooney, W.; Biegler, L.; Glasser, D.; Hildebrandt, D. Linear Programming Formulations for Attainable Region Analysis. *Chem. Eng. Sci.* **2002**, *57*, 2015.

(56) Abraham, T.; Feinberg, M. Kinetic Bounds on Attainability in the Reactor Synthesis Problem. *Ind. Eng. Chem. Res.* **2004**, *43*, 449.

(57) Zhou, W.; Manousiouthakis, V. Non-Ideal Reactor Network Synthesis Through IDEAS: Attainable Region Construction. *Chem. Eng. Sci.* **2006**, *61*, 6936.

(58) Zhou, W.; Manousiouthakis, V. Variable Density Fluid Reactor Network Synthesis: Construction of the Attainable Region Through the IDEAS Approach. *Chem. Eng. J.* **2007**, *129*, 91.

(59) Rippin, D. Simulation of Single- and Multi-Product Batch Chemical Plants for Optimal Design and Operation. *Comput. Chem. Eng.* **1983**, *7*, 137.

(60) Rippin, D. W. T. Design and Operation of Multi-product and Multi-purpose Batch Chemical Plants. *Comput. Chem. Eng.* **1983**, *7*, 463.

(61) Rippin, D. Batch Process Systems Engineering: A Retrospective and Prospective Review. *Comput. Chem. Eng.* **1993**, *17*, S1.

(62) Reklaitis, G. V. *Progress and Issues in Computer-Aided Batch Process Design: from Foundations of Computer-Aided Process Design*; Elsevier: New York, 1990.

(63) Levien, K. Maximizing the Product Distribution in Batch Reactors: Reactions in Parallel. *Chem. Eng. Sci.* **1992**, *47*, 1751.

(64) Terwiesch, P.; Agarwal, M.; Rippin, D. Batch Unit Optimization with Imperfect Modeling: A Survey. *J. Process Control* **1994**, *4*, 238.

(65) Yi, G.; Reklaitis, G. Optimal Design of Batch-Storage Network with Recycle Streams. *AIChE J.* **2003**, *49*, 3084.

(66) Maravelias, C. A Decomposition Framework for the Scheduling of Single- and Multi-Stage Processes. *Comput. Chem. Eng.* **2006**, *30*, 407.

(67) Sung, C.; Maravelias, C. An Attainable Region Approach for Production Planning of Multi-Product Processes. *AIChE J.* **2007**, *53*, 1298.

(68) Levenspiel, O. *Chemical Reaction Engineering*; Wiley: New York, 1972.

(69) Froment, G.; Bischoff, K. *Chemical Reactor Analysis and Design*; Wiley: New York, 1979.

(70) Schmidt, L. *Engineering of Chemical Reactions*; Oxford University Press: New York, 1998.

(71) Fogler, H. S. *Elements of Chemical Reaction Engineering*; Prentice Hall: Upper Saddle River, NJ, 1999.

(72) Nauman, E. B. *Chemical Reactor Design, Optimization, and Scaleup*; McGraw-Hill: New York, 2002.

(73) Rawlings, J.; Ekerdt, J. *Chemical Reactor Analysis and Design Fundamentals*; Nob Hill Publishing: Madison, WI, 2002.

(74) Zhang, J.; Smith, R. Design and Optimization of Batch and Semi-Batch Reactors. *Chem. Eng. Sci.* **2004**, *59*, 459.

(75) Khalil, H. K. *Nonlinear Systems*; Prentice Hall: Upper Saddle River, NJ, 1996.

(76) Justanieah, A. On the Convergence of a Finite-Dimensional Approximation Algorithm for a Class of Infinite-Dimensional Linear Programs: An Application to the IDEAS Framework, Ph.D. Thesis, University of California at Los Angeles (UCLA), Los Angeles, CA, 2004.

(77) Bapat, R. B.; Raghavan T. E. S. *Non-Negative Matrices and Applications: Encyclopedia of Mathematics and its Applications*; Cambridge University Press: New York, 1997.

(78) Cormen, T. H.; Leiserson, C. E.; Rivest, R. L. *Introduction to Algorithms*; McGraw−Hill: New York, 1990.

(79) Trambouze, P.; Piret, E. Continuous Stirred Tank Reactors: Designs for Maximum Conversions of Raw Material to Desired Product: Homogeneous Reactions. *AIChE J.* **1959**, *5*, 384.

Received for review December 5, 2007
Revised manuscript received March 10, 2008
Accepted March 11, 2008

IE071664L